

Nucleotide excision repair–initiating proteins bind to oxidative DNA lesions in vivo

Hervé Menoni, Jan H.J. Hoeijmakers, and Wim Vermeulen

Department of Genetics, Erasmus MC, 3015 GE Rotterdam, Netherlands

Base excision repair (BER) is the main repair pathway to eliminate abundant oxidative DNA lesions such as 8-oxo-7,8-dihydroguanine. Recent data suggest that the key transcription-coupled nucleotide excision repair factor (TC-NER) Cockayne syndrome group B (CSB) and the global genome NER-initiating factor XPC are implicated in the protection of cells against oxidative DNA damages. Our novel live-cell imaging approach revealed a strong and very rapid recruitment of XPC and CSB to sites of oxidative DNA lesions in living cells. The absence of detectable accumulation of downstream NER

factors at the site of local oxidative DNA damage provide the first in vivo indication of the involvement of CSB and XPC in the repair of oxidative DNA lesions independent of the remainder of the NER reaction. Interestingly, CSB exhibited different and transcription-dependent kinetics in the two compartments studied (nucleolus and nucleoplasm), suggesting a direct transcription-dependent involvement of CSB in the repair of oxidative lesions associated with different RNA polymerases but not involving other NER proteins.

Introduction

DNA is constantly damaged by numerous chemicals, ionizing radiation (IR), or ultra-violet (UV) light. However, a significant fraction of DNA lesions is derived from endogenous genotoxic agents constituting a major threat for genome stability. For instance, reactive oxygen species (ROS) generated by aerobic metabolism can lead to oxidation of nucleobases in DNA. Guanine (G), due to its lower redox potential compared with other DNA bases, is the main target for oxidation, which produces one of the most abundant DNA lesions: 8-oxo-7,8-dihydroguanine (8-oxoG). The frequency of abundant lesions such as 8-oxoG is estimated to vary between ~ 0.1 and 1 lesion per million bases, depending on the method used and the cells studied (Cadet et al., 2011). Despite variations in detection, the amount of 8-oxoG remains several times higher than another class of bulky oxidative lesions, such as 8,5'-cyclopurine-2'-deoxynucleosides that are present in only 0.02 lesion per million bases (Kirkali et al., 2009). 8-oxoG can mispair with adenine and

thereby introduce G:C to T:A transversions during replication (Shibutani et al., 1991; Moriya, 1993). This miscoding potential of 8-oxoG contributes to spontaneous mutations and may ultimately trigger carcinogenesis (Maynard et al., 2009). Moreover, 8-oxoG can cause transcriptional mutagenesis, which may have important implications for tumorigenesis (Saxowsky et al., 2008). Oxidative DNA lesions are also thought to be involved in a broad spectrum of human pathogenesis related to aging, such as neurodegenerative diseases (Sedelnikova et al., 2010).

To repair abundant endogenously produced DNA damages like 8-oxoG, cells use the base excision repair (BER) pathway (Hegde et al., 2008). This in vitro well-characterized BER is initiated by lesion-specific glycosylases that recognize the damage and remove the affected base from the sugar-phosphate backbone. Subsequently, the backbone is incised, the remaining apurinic-apyrimidinic site removed, and the single nucleotide gap filled by a specific DNA polymerase (DNA polymerase β) and finally sealed by ligation. Different glycosylases initiate repair of 8-oxoG, with OGG1 as the major one (Radicella et al., 1997; Rosenquist et al., 1997).

Correspondence to Hervé Menoni: h.menoni@erasmusmc.nl; or Wim Vermeulen: w.vermeulen@erasmusmc.nl

Abbreviations used in this paper: 6-4PP, 6-4 pyrimidine-pyrimidone photoproducts; 8-oxoG, 8-oxo-7,8-dihydroguanine; ActD, Actinomycin D; BER, base excision repair; CPD, cyclo-butane pyrimidine dimer; CSB, Cockayne syndrome group B; DSB, double-strand break; GG-NER, global genome nucleotide excision repair; IF, immunofluorescence; NER, nucleotide excision repair; NMR, nuclear magnetic resonance; OGG1, 8-oxoguanine DNA glycosylase; RNAP, RNA polymerase; ROS, reactive oxygen species; SSB, single-strand break; TC-NER, transcription-coupled nucleotide excision repair; UV, ultra-violet; XP, xeroderma pigmentosum group.

© 2012 Menoni et al. This article is distributed under the terms of an Attribution–Noncommercial–Share Alike–No Mirror Sites license for the first six months after the publication date [see <http://www.rupress.org/terms>]. After six months it is available under a Creative Commons License [Attribution–Noncommercial–Share Alike 3.0 Unported license, as described at <http://creativecommons.org/licenses/by-nc-sa/3.0/>].

Nucleotide excision repair (NER) removes more helix-destabilizing lesions, like the UV light-induced 6-4PPs and CPDs, intrastrand cross-links, and numerous bulky chemical adducts. Moreover, some bulky oxidative lesions, e.g., 8,5'-cyclopurine-2'-deoxynucleosides, are also eliminated by NER. NER utilizes more than 25 proteins to remove lesions by excising a patch of ~22–30 nucleotides. Initiation of the two NER subpathways, global genome NER (GG-NER) and transcription-coupled NER (TC-NER), requires UV-DDB and XPC and the CSA and CSB proteins, respectively (Hanawalt and Spivak, 2008; Lagerwerf et al., 2011; Naegeli and Sugasawa, 2011).

Direct functioning of NER or a cross talk between NER and BER to repair “non-bulky” oxidative DNA lesions was suggested in several studies. XPC was proposed to play a role in the protection of cells against oxidative DNA damages (D’Errico et al., 2006; Kassam and Rainbow, 2007; Melis et al., 2008, 2011). Even more evidence has been collected for the involvement of CSB in the response to oxidative DNA damages (Stevnsner et al., 2008). However, the exact molecular function of these two NER factors in the repair of oxidative DNA lesions remains elusive. Moreover, conflicting data and models are presented, such as that CS-B cellular extracts exhibit reduced incision activity on a naked DNA (non-nucleosomal) 8-oxoG substrate (Dianov et al., 1999; Tuo et al., 2002), which could not be confirmed by others (Osterod et al., 2002), likely due to experimental variations. Recently, *in vitro* analyses of 8-oxoG repair using a chromatinized template have shown that the chromatin structure regulates repair efficiency of this lesion, emphasizing the importance to study DNA repair in its natural context, i.e., the living cell (Menoni et al., 2007, 2012).

To further investigate 8-oxoG repair in intact living cells and to disclose whether the NER initiators XPC and CSB are implicated, we describe here the development of a novel laser-assisted procedure to locally inflict oxidative DNA lesions. The observed *in vivo* binding of CSB and XPC to these oxidative DNA lesions provides evidence for a direct role of these factors in the repair of such lesions. CSB exhibited a prominent localization in the nucleolus, whereas XPC accumulated more abundantly in DNA-dense (heterochromatic) subnuclear areas. Surprisingly, however, this initial recruitment of XPC and CSB does not trigger a canonical NER reaction as none of the downstream NER factors appeared to be detectably recruited. In addition, we observed a strong link with transcription for the CSB binding to lesions, indicative of a transcription-associated process in the response of CSB to oxidative lesions.

Results and discussion

XPC and CSB are recruited to oxidative DNA lesions *in vivo*

To investigate whether CSB and XPC are involved in the repair of oxidative DNA lesions, we used a live-cell imaging approach combining the expression of fluorescently tagged, functional XPC and CSB (see Materials and methods) with a novel procedure to locally inflict oxidative DNA damage. The generation of oxidative DNA damage, predominantly 8-oxoG lesions in cultured cells, is based on using the photosensitizer Ro 19-8022 in combination with white lamp illumination (Will et al., 1999).

To generate oxidative DNA damage in a discrete region in nuclei of cultured cells, we used a constant wave 405-nm laser that generates the energy required for local photo-activation of Ro 19-8022 (detailed in Materials and methods). Antibodies that specifically recognize 8-oxoG (Amouroux et al., 2010) confirmed that indeed this DNA lesion is locally inflicted (Fig. S1 A). In cells expressing functional OGG1-DsRed a significant local accumulation of this 8-oxo-G glycosylase within the laser-irradiated spot was observed (Fig. 1 A). This novel laser-assisted procedure does not induce detectable amounts of double strand breaks (DSBs), as shown by the Ku-80 DSB marker (Mari et al., 2006), nor the UV-lesions CPDs or 6-4PPs (classical NER-substrates; Fig. S1, B–D; Dinant et al., 2007). Surprisingly, both XPC-GFP and GFP-CSB were recruited to the region where the laser was directed in the presence of photosensitizer (Fig. 1, B and C, arrows), whereas in its absence no prominent enrichment for XPC or CSB was observed. The only weak accumulation of XPC in the absence of photosensitizer (Fig. 1 C, asterisk) contrasts with the strong accumulation to oxidative DNA damages of both endogenous XPC and the fluorescently tagged version (Fig. 1 C, arrow; and Fig. S1 E). This suggests that XPCs bind much better oxidative base damage than direct SSBs, as suggested also by a previous study (Lan et al., 2004; Fig. S1 F).

The accumulation of XPC and CSB was clearly visible immediately after the DNA damage infliction. To measure the initial binding kinetics of XPC and CSB to local 8-oxoG we increased the photosensitizer concentration, allowing minimal illumination time. The recruitment of CSB appeared slightly faster than that of XPC (Fig. 1 D), whereas OGG1 binding appeared to precede CSB (Fig. S1 G). The delay of XPC might be explained by the intrinsic slow mobility properties of XPC, caused by a continuous transient interaction with undamaged DNA (Hoogstraten et al., 2008). Alternatively, the slight delayed binding of XPC might be to OGG1-generated AP sites, created by the relatively fast glycosylase activity of OGG1 as compared with its AP-lyase activity (Zharkov et al., 2000). The AP site induces a stronger helix distortion than 8-oxoG, and is thus likely to be sensed by XPC (Sági et al., 2001). However, silencing OGG1 expression didn’t abrogate the recruitment of XPC or CSB (Fig. S1 H), suggesting that the binding of both NER factors is to 8-oxoG, and not to an early BER intermediate. Nevertheless, incomplete silencing (leaving trace amounts of active OGG1) and other (partly redundant) glycosylases functioning as backup for OGG1 depletion leaves the AP site as a possible XPC target. Previous structural studies suggested that 8-oxoG does not induce strong helix destabilization (Oda et al., 1991; Lipscomb et al., 1995) as the canonical XPC (NER) substrates (Naegeli and Sugasawa, 2011). However, recent thermodynamic and NMR analysis suggested that 8-oxoG destabilizes the DNA helix by inducing changes in the hydrophilicity of the base and impacting on the major groove cation binding (Singh et al., 2011) rendering this lesion as a directly XPC-recognizable target.

The accumulation of CSB remains visible even a few hours after damage induction (Fig. 1 E), in accordance with previously reported BER kinetics of oxidative DNA damage (Will et al., 1999; Amouroux et al., 2010). The lasting accumulation of XRCC1 and OGG1 after 30 min further confirms that our locally generated oxidative base damage triggers a conventional

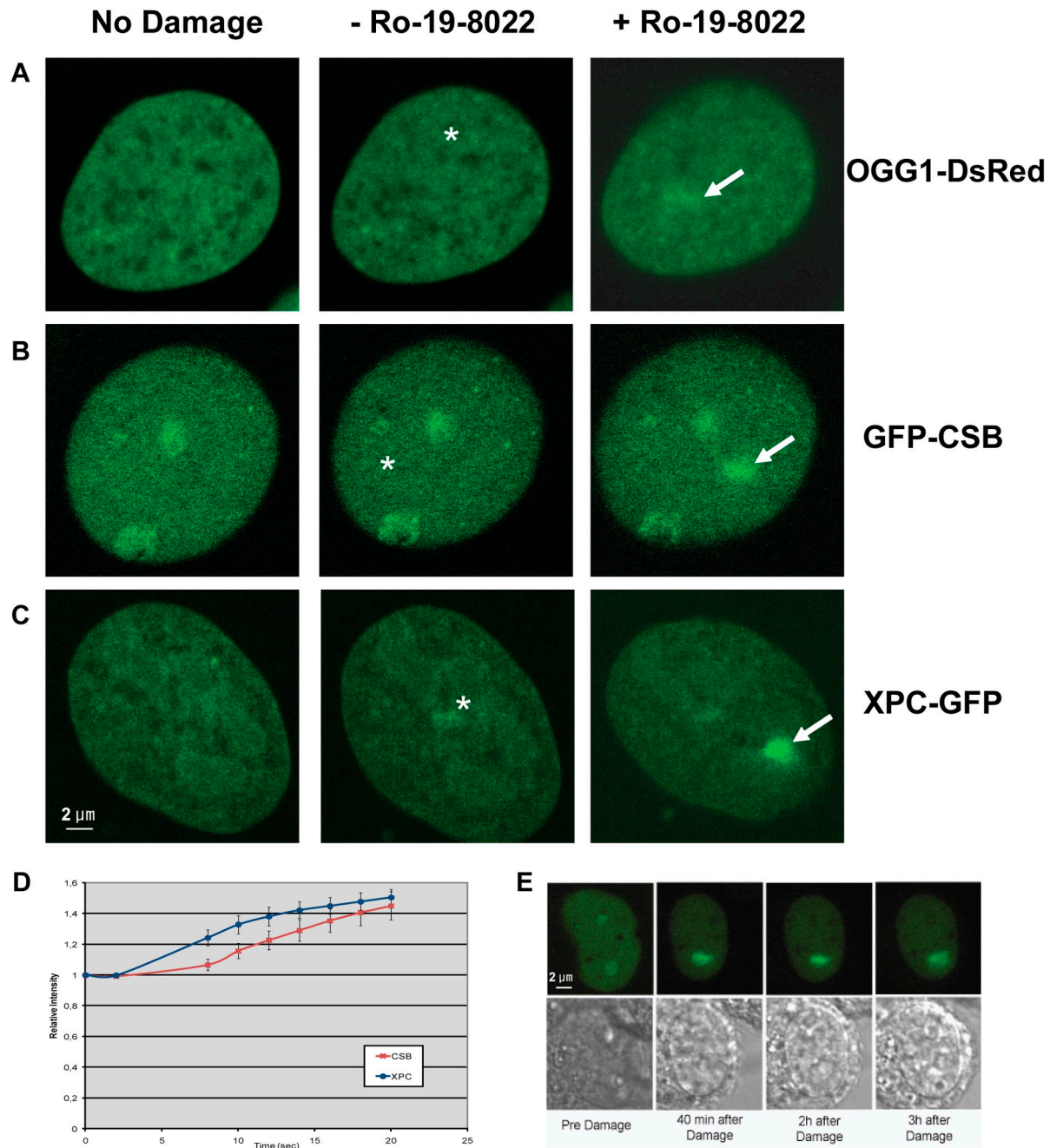


Figure 1. **GG-NER and TC-NER initiating factors are recruited to oxidative DNA lesions in vivo.** (A) CS1AN-Sv fibroblast stably expressing OGG1-DsRed. (B) CS1AN-Sv fibroblast stably expressing GFP-CSB. (C) XP4PA-Sv fibroblasts stably expressing XPC-GFP. (A–C) Left row, before DNA damage induction; middle row, locally irradiated with 405-nm laser (*); right row, locally irradiated with 405-nm laser plus photosensitizer RO-19-8022 (arrow). (D) Accumulation kinetics of XPC-GFP and GFP-CSB (error bars indicate SEM of >7 cells). (E) Time series showing the persistence of GFP-CSB accumulation on local oxidative DNA damage. Top row, GFP-signal; bottom row, the corresponding phase-contrast images.

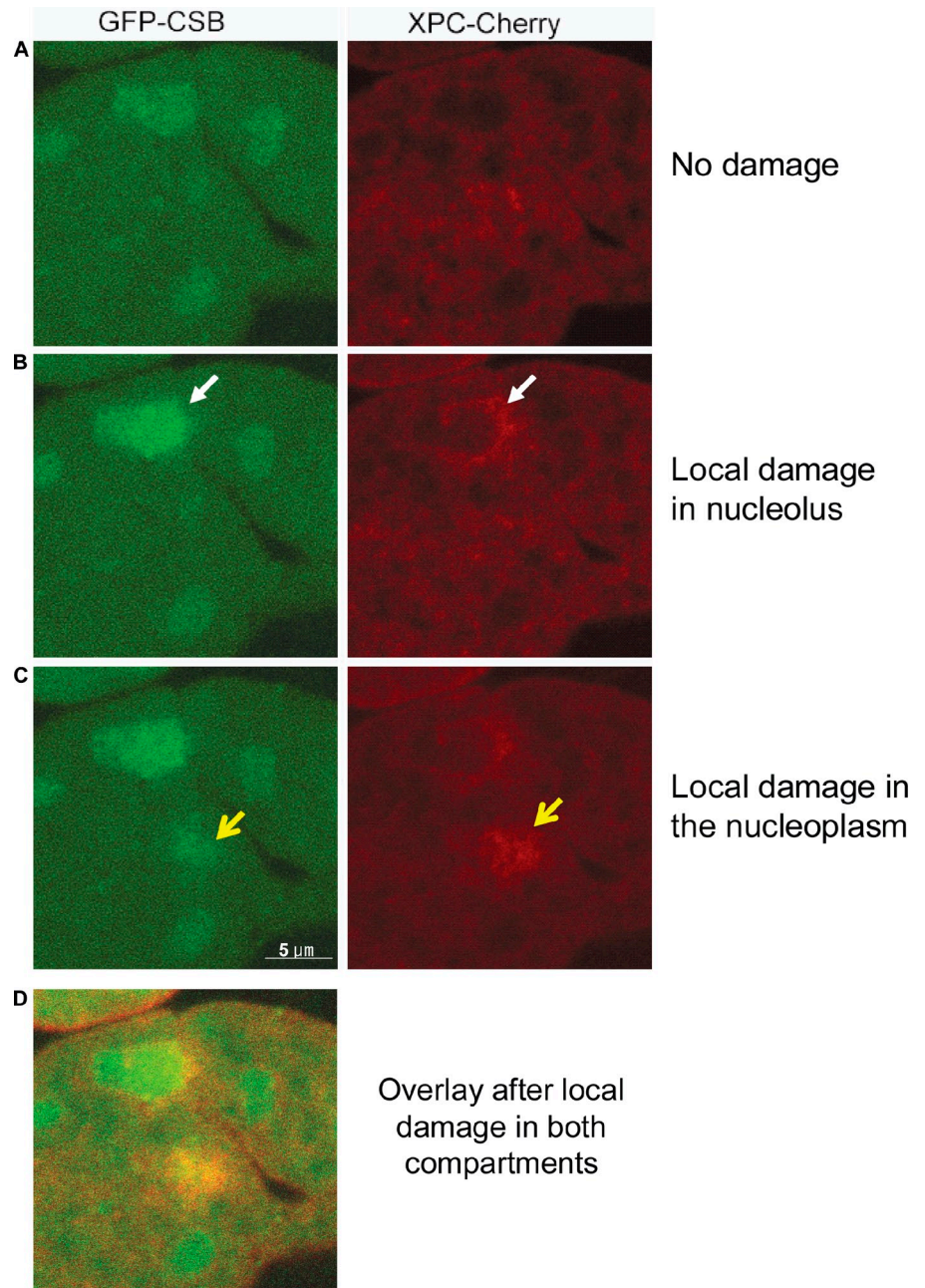
BER (Fig. S1 I). The persistent accumulation of CSB (Fig. 1 E) further confirms that these proteins bind to 8-oxoG as opposed to direct SSBs because these are swiftly repaired in less than 30 min (Mortusewicz and Leonhardt, 2007).

Accumulation of XPC and CSB without inducing NER

The clear accumulation of factors initiating both NER sub-pathways on local oxidative DNA damage prompted us to

monitor whether other NER factors also accumulate. We concentrated on proteins acting directly downstream in both NER sub-pathways: XPB (TFIIH subunit), implicated in helix opening after damage detection; and XPA, which assists TFIIH in damage verification and further organization of the NER complex. We used cell lines that stably express biological functional GFP-XPA and XPB-GFP (see Materials and methods) and monitored the recruitment both immediately after and 5–10 min after DNA damage infliction. Remarkably, in contrast to both XPC and

Figure 2. **Binding of CSB and XPC to oxidative DNA lesions in different nuclear compartments.** (A) Co-expression of XPC-Cherry and CSB-GFP in XPC fibroblasts. In the absence of damage GFP-CSB is enriched in the nucleolus, whereas XPC-Cherry appeared less abundant in this compartment. (B) GFP-CSB is strongly enriched at oxidative DNA damage in the nucleolus (white arrows), whereas XPC-Cherry is not visibly enriched but shows more accumulation in the heterochromatic perinucleolar region surrounding the nucleolus. (C) A second local DNA damage in the nucleoplasm (yellow open arrows) shows homogenous recruitment for both factors. (D) A second local DNA damage in the nucleoplasm (yellow open arrows) shows homogenous recruitment for both factors.



CSB, none of these NER factors were significantly recruited to oxidative DNA damages generated in our setting (unpublished data). We conclude that although NER initiation factors accumulate on oxidative DNA damage, they do not trigger a canonical NER reaction. Because no NER is induced on these lesions, but the previous cellular studies (Osterod et al., 2002; D'Errico et al., 2006) suggested a function of both these proteins in the response to oxidative damage, we tested whether they were implicated in BER. In human fibroblasts deficient for either XPC or CSB the accumulation of OGG1-DsRed disappeared faster than in wild-type cells (Fig. S1, compare J and K with I). This different behavior of OGG1 (less stably bound as compared with wild-type cells) indicates that the BER reaction is changed and is in line with previous observations suggesting that CSB functions in coordinating or fine-tuning the BER reaction (Khobta et al., 2009).

Differential intranuclear spatial recruitment of XPC and CSB

We attributed the different binding kinetics of XPC and CSB to local oxidative DNA damage to their respective diffusion and overall chromatin-binding properties. In addition, both proteins exhibit differential distribution patterns in nuclei of cells that did not receive exogenous DNA damage; XPC follows a typical chromatin/DNA distribution pattern, whereas CSB presents a diffuse nuclear distribution in addition to enrichment in the nucleolus (see Fig. 3 A) (Bradsher et al., 2002; van den Boom et al., 2004; Hoogstraten et al., 2008). This high local concentration of CSB in nucleoli correlates with the high RNAPI-driven transcriptional activity in this nuclear compartment in which CSB was suggested to function (Bradsher et al., 2002; Yuan et al., 2007). To investigate if the recruitment of CSB and XPC

to local oxidative DNA lesions was different in various subnuclear compartments with different transcriptional activities, we used the nucleolus as a center of high transcription. The nucleolus is easily detectable in these cells with transmission optics and may represent in proliferating cells more than 50% of the total cellular transcription (Grummt and Ladurner, 2008). To compare simultaneously the behavior of CSB and XPC in living cells we coexpressed the two proteins with two different fluorescent markers (GFP-CSB and XPC-mCherry). Both fluorescent proteins showed the expected distribution patterns, with nucleolar-depleted XPC-mCherry and enriched GFP-CSB (Fig. 2 A). The nucleolus is surrounded by dense heterochromatin where XPC-Cherry is visibly enriched (Fig. 2 B).

We observed a strong enrichment of GFP-CSB after local damage induction in the nucleolus, whereas XPC-Cherry accumulation was not visibly enhanced, though this protein was clearly elevated in the heterochromatin surrounding the nucleolus, where GFP-CSB was low, yielding a complementary picture of CSB and XPC accumulation (Fig. 2 D). When we induced local oxidative DNA damage (with the same settings) in the nucleoplasm of the same nucleus a much stronger and more homogeneous enrichment of XPC-Cherry in comparison with the nucleolus became apparent (Fig. 2 C). Quantification of the relative amount of accumulated proteins confirmed that XPC-mCherry was less abundantly enriched in the nucleolus as compared with nucleoplasm, though clearly quantifiable (Fig. S2 A). In contrast, the relative recruitment of GFP-CSB is similar outside or inside the nucleolus (Fig. S2 B), suggesting that this recruitment is not simply dependent on the total DNA content of the intranuclear region. OGG1-DsRed was recruited to local oxidative DNA damage in the nucleolus, though to a lesser extent than in the nucleoplasm, as for XPC (Fig. S2 C). It is very likely that the lower DNA content, and thus a lower amount of lesions, are explaining this pattern of OGG1 (Fig. S2 D). The stronger accumulation of GFP-CSB in nucleoli may suggest that CSB is mainly targeted to transcriptionally active sites. To the contrary, the XPC recruitment to damaged DNA seems independent of the transcriptional status and the lower amount of recruited protein in nucleoli is in accordance with the relatively low DNA content in this subnuclear compartment.

Differential CSB mobility in the nucleoplasm versus the nucleolus

To measure protein mobility, we used an adapted FRAP method (Houtsmuller and Vermeulen, 2001; see Materials and methods and Fig. S3 A). As shown in Fig. 3 A, the mobility of CSB in the nucleolus is lower than elsewhere in the nucleus. In the nucleoplasm the majority of CSB was already exchanged in less than 2 s, whereas it took more than 5 s for a similar recovery in the nucleolus. Full recovery of fluorescence of GFP-CSB in the nucleolus is reached only after ~25 s (Fig. 3 B). Interestingly, these data are similar to the previously observed residence times for TFIIH when respectively involved in RNAPII and RNAPI transcription (Hoogstraten et al., 2002) and suggest that these differential mobilities of CSB reflect the transient interaction with the two RNAPs. The reduced mobility of CSB in the nucleolus (Fig. 3 A) may reflect a previously suggested role of

CSB in RNAPI transcription (Bradsher et al., 2002; Yuan et al., 2007). However, the mobilities of several RNAPI components recently published are lower than CSB and would argue for a transient interaction of CSB with RNAPI (Gorski et al., 2008), suggesting that CSB is only an accessory RNAPI factor, which is in line with the notion that in its absence, transcription of rDNA is reduced but not abolished (Yuan et al., 2007).

Nucleolar oxidative DNA damage induced immobilization of GFP-CSB

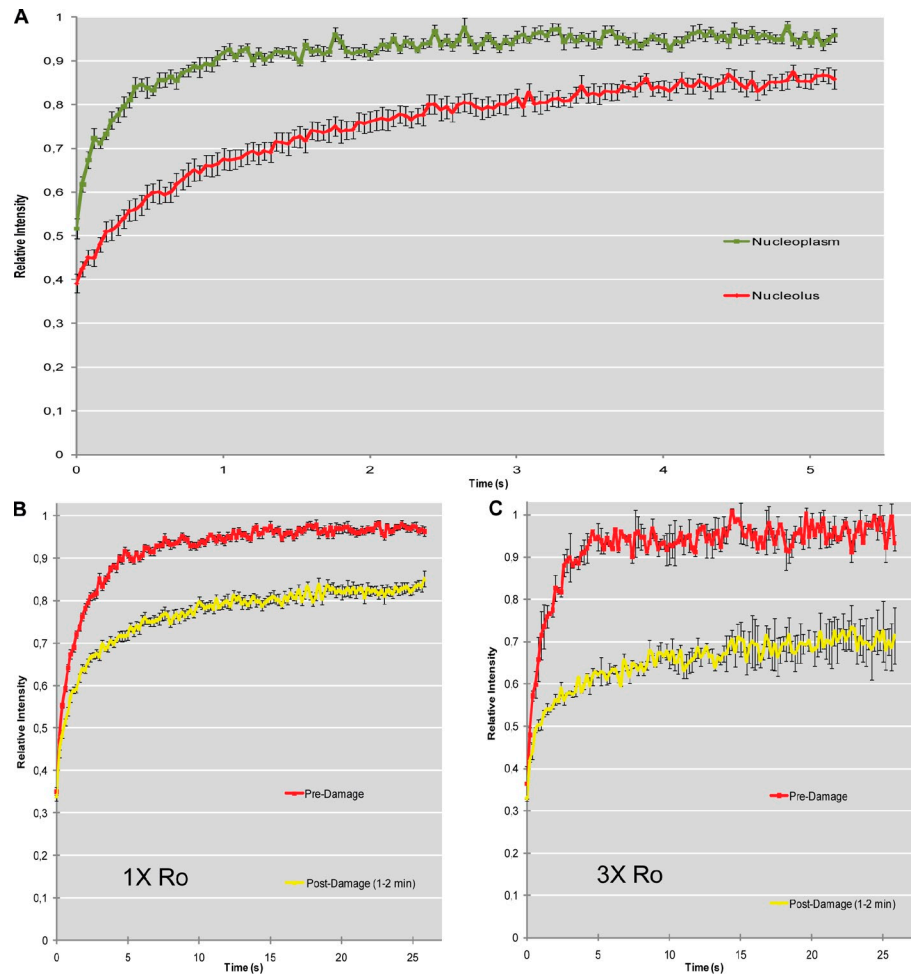
The abundant accumulation of CSB within nucleoli to oxidative DNA damage (Fig. 2 B) prompted us to examine whether oxidative DNA damage affects mobility of the protein. FRAP data shown in Fig. 3 B reveal an incomplete fluorescence recovery beyond 25 s after bleaching (the approximate time for full recovery in the nondamaged situation), which indicates that in the presence of oxidative DNA damage a fraction of GFP-CSB molecules is temporarily trapped in the nucleolus. The amount of transiently immobilized GFP-CSB in the nucleolus increases with increasing dose of photosensitizer (Fig. 3, compare B and C) displaying a dose–response relationship in accordance with an increased amount of 8-oxoG detected by IF (Fig. S2, D and E). Together these results suggest that the immobilization of GFP-CSB reflects actual participation of this protein in a “DNA-bound process” on oxidative lesions. Although this mobility change is not a direct proof for CSB acting on oxidative damage, it is consistent with the idea that CSB helps RNAPI to cope with oxidative DNA lesion, either by promoting translesion transcription or actual removal of the damage. The recruitment of CSB to oxidative lesions in the nucleolus is in concordance with previous data, which showed that CSB can favor transcriptional mutagenesis on 8-oxoG lesions (Saxowsky et al., 2008) and that it is also implicated in reducing the steady-state level of 8-oxoG (Osterod et al., 2002).

Oxidative DNA lesions immobilize CSB in a transcription-dependent manner

Although oxidative DNA damage induced a robust accumulation and immobilization of CSB in the nucleolus (Figs. 3 and 4), we also noted a clear recruitment of GFP-CSB to local oxidative DNA damage in the nucleoplasm. To test whether CSB is recruited and bound to the oxidative lesions with similar kinetics in the nucleoplasm as in the nucleolus, we targeted the 405-nm laser (in the presence of the photosensitizer) in the nucleoplasm and monitored the mobility of CSB. We observed a strikingly similar immobilized fraction of GFP-CSB in the nucleoplasm and in the nucleolus (Fig. 4 A). Despite rather diverse mobility parameters of GFP-CSB between nucleolus and nucleoplasm, these data show that in both compartments CSB responds with similar kinetics to oxidative damage, arguing for a common mechanism.

We propose that the relative slow mobility of GFP-CSB in the nucleolus is caused by transient interactions with the RNAPI transcription machinery. An alternative explanation is, however, that the diffusion of GFP-CSB is hindered by a possible denser environment in this compartment. To test this we studied the mobility of XPC in the nucleolus. Although XPC is much less

Figure 3. Differential CSB mobility in the nucleoplasm versus the nucleolus. (A–C) FRAP analysis of GFP-CSB in the nucleolus and nucleoplasm, in the absence and presence of oxidative DNA damage. (A) Mobility of GFP-CSB, in the absence of oxidative DNA damage, is higher (full recovery in ~2–3 s) in the nucleoplasm (green curve) than in the nucleolus (red curve). (B) Oxidative damage (405 nm with 500 nM RO-19-8022) in the nucleolus significantly decreased the GFP-CSB mobility (yellow curve) as compared with nondamaged nucleoli (red curve). Mean and SEM of >8 cells. The incomplete recovery beyond 25 s after bleaching represents a transient immobilized fraction. (C). In the presence of three times more photosensitizer a larger fraction of GFP-CSB is immobilized (compare yellow lines in B and C). Mean and SEM of two cells.



abundant in the nucleolus, its fluorescent signal is sufficient to apply the same FRAP procedure. In both compartments XPC-GFP exhibited identical mobility (Fig. 4 B), suggesting that neither the density nor the presence of fibrous structures within the nucleolus slows down the mobility of proteins.

The above analyses suggest that—in contrast to XPC—CSB mobility parameters and binding characteristics to oxidative damage are (in part) determined by the nuclear localization. One particular feature of the nucleolus is its high (RNAPI) transcriptional activity, and we thus propose that CSB binding to oxidative DNA damage is transcription dependent. To further show that a transcription-associated process determines binding of CSB to oxidative DNA damage, we used a transcription inhibitor for both RNAPI and RNAPII, Actinomycin D (ActD). When inhibiting transcription with ActD the distribution of CSB-GFP is changed especially in the nucleolus (Fig. S3 B). Despite this change, CSB is still recruited in the presence of the intercalator and 8-oxoG is normally formed (Fig. S2, D and E). FRAP analysis of CSB inside (Fig. 5 A) or outside (Fig. 5 B) the nucleolus shows that the immobilized fraction was significantly reduced when we applied the same type of local oxidative DNA damages as in Fig. 4. ActD intercalates in DNA and impedes RNAPs to elongate. So we conclude that the fraction of CSB engaged in active transcription, and interacting with the RNAPI or RNAPII is the major fraction of CSB implicated in dealing with oxidative DNA damage.

Although CSB appeared to be involved in processing of oxidative lesions in an RNAPI-dependent fashion, our studies do not discriminate whether the action of CSB is strand specific or not, as in the case of TC-NER (Lagerwerf et al., 2011). Previously, 8-oxo-G was shown to interfere with transcription when the lesion is located in the transcribed as well as in the nontranscribed strand (Kitsera et al., 2011). It is also possible that CSB creates a chromatin environment, permissive for efficient transcription and DNA repair (Citterio et al., 2000), irrespective of the DNA strand. It is currently even disputed whether 8-oxo-G lesions give rise to RNAP stalling, as with bulky NER lesions, because different studies provide conflicting results, ranging from weak transcriptional interference to complete absence of an effect (Tornaletti et al., 2004; Charlet-Berguerand et al., 2006; Spivak and Hanawalt, 2006; Khobta et al., 2009). Here we show that recruitment and retention of CSB to oxidative DNA damage in vivo depends on transcription and may reflect an active role of CSB in DNA repair. Alternatively, CSB may not directly be involved in BER, but may stimulate transcription efficiency when confronted with oxidative DNA lesions.

Here we present a novel procedure to specifically generate oxidative DNA damage in only a small part of the nucleus on a user-defined position. Combining this new method with a live-cell imaging approach allowed us to analyze the recruitment of DNA repair proteins to oxidative DNA damage in the nucleolus

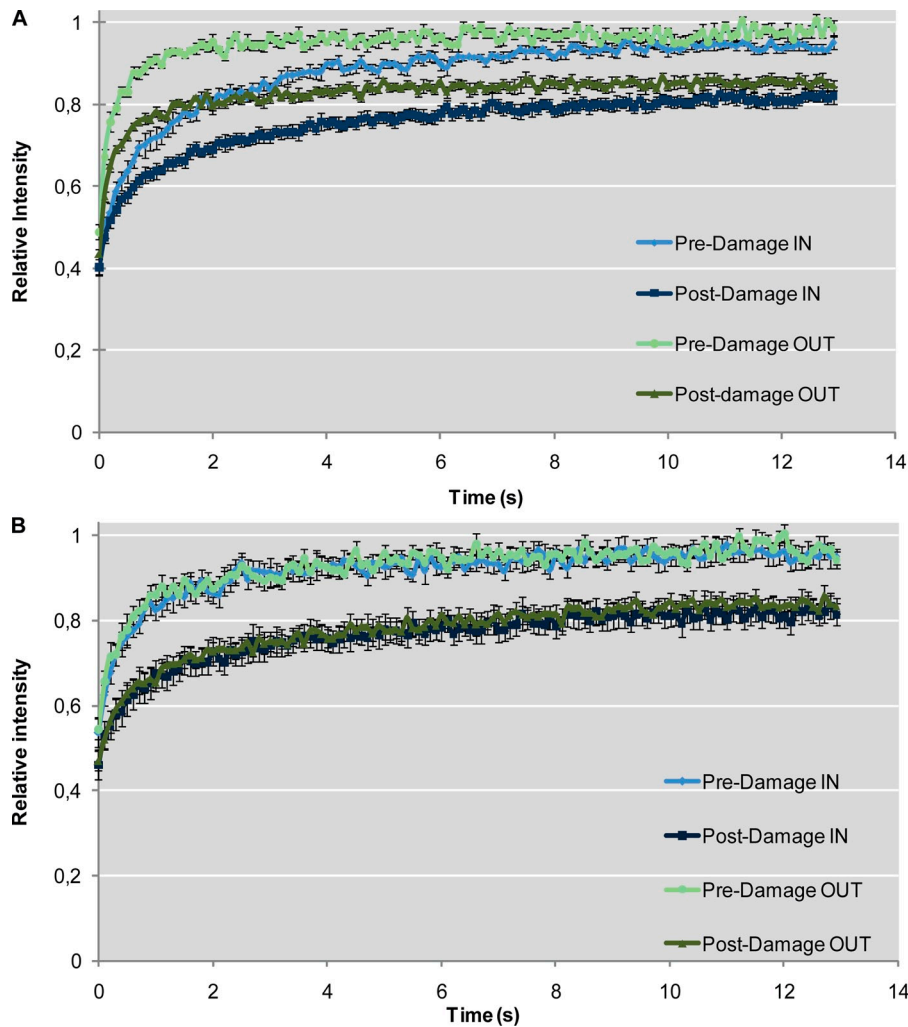


Figure 4. Oxidative damage-induced mobility of CSB and XPC in different nuclear compartments. (A) FRAP analysis of GFP-CSB in nucleolus (blue) and nucleoplasm (green) before (bright colors) and after (dark colors) oxidative DNA damage. (B) FRAP analysis of XPC-GFP in nucleolus (blue) and nucleoplasm (green) before (bright colors) and after (dark colors) oxidative DNA damage. FRAP curves are from >10 cells, error bars represent SEM.

and in the nucleoplasm. We focused on two NER factors, CSB and XPC, which were, by indirect approaches, recently suggested to play a role in the repair of 8-oxoG. Our data show for the first time in vivo recruitment of CSB and XPC to 8-oxoG. The immobilization of these factors in addition to the absence of a clear XPA or XPB accumulation suggests that XPC and CSB have a direct role in the repair of oxidative DNA damage outside of their classical involvement in the NER pathway. CSB exhibited a prominent recruitment when the DNA damage is in the nucleolus, whereas XPC accumulated more abundantly in DNA-dense (heterochromatic) areas of the nucleoplasm. The prominent recruitment of CSB in the nucleolus to 8-oxoG and the reduced immobilization upon transcription inhibition suggests the existence of a transcription-associated repair of this lesion mediated by CSB.

Materials and methods

Cell lines

We used several fibroblast cell lines derived from patients and corrected for the NER deficiency by stably expressing an EGFP fusion of the defective protein. Cell lines used in this study were SV40 immortalized human fibroblasts, XPC deficient (xeroderma pigmentosum group C [XP-C]) XP4PA-SV WT, or expressing XPC-EGFP (Politi et al., 2005); the CS1AN-SV (Cockayne syndrome group B [CS-B]) expressing EGFP-CSB (van den Boom et al., 2004); XP12RO-SV (XP-A) expressing EGFP-XPA (Rademakers et al., 2003); and XPCS2BA-SV (XP-B) expressing XPB-EGFP (Hoogstraten et al., 2002).

For the EGFP-CSB fusion construct full-length N-terminally HA-tagged CSB cDNA was cloned in frame in pEGFP-C3 using SacI-SalI sites. The full-length human XPC cDNA was cloned in frame in pEGFP-N3 that contains a C-terminal His₆-HA tag inserted in SspBI-NotI site to generate the XPC-EGFP expression construct. The EGFP-XPA fusion cDNA was obtained by inserting the XPA cDNA fragment (nucleotides 9–863) in a pEGFP-C1 vector that harbors a His₆-HA tag at the N terminus of GFP. Full-length XPB cDNA was cloned in frame into the pEGFP-N1 vector to generate the C-terminal fusion of XPB with EGFP. HeLa and XR-V15B cells stably expressing EGFP-Ku-80 were a gift of Dik C. van Gent (Erasmus MC, Rotterdam, Netherlands; Mari et al., 2006). All cell lines were grown in a 1:1 mixture of Ham's F10 and DMEM (Gibco) supplemented with antibiotics and 10% FCS at 37°C, 5% CO₂.

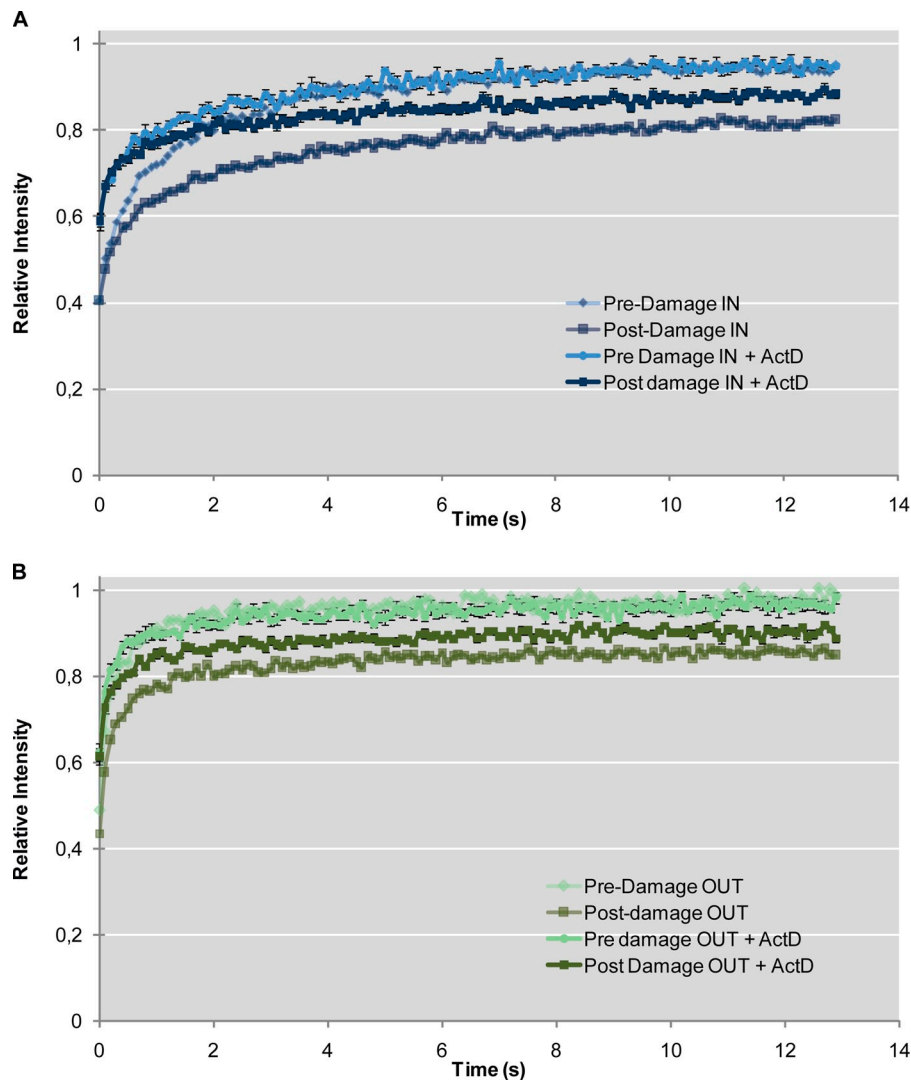
Transient expression of fusion proteins and cell transfection

We used plasmid containing XPC-mCherry (Bergink et al., 2012), EGFP-CSB (van den Boom et al., 2004), OGG1-DsRed, and XRCC1-YFP (gifts of A. Campalans and J.P. Radicella, CEA, Institute of Cellular and Molecular Radiobiology, Fontenay aux Roses, France; Amouroux et al., 2010) fusion for the transient transfections. Transient transfections were performed using FuGENE transfection reagent (Roche) according to the manufacturer's instructions. The double expression allows a qualitative and robust comparison of recruitment at the same local DNA damages avoiding any intra-experimental and intra-cell variation. Silencing of human OGG1 was done with ON-TARGETplus SMARTpool L-005147-00-0005 (Thermo Fisher Scientific) transfected with Lipofectamine RNAiMAX reagent (Invitrogen) according to the manufacturer's instructions.

Immunofluorescence

We checked for the presence of CPDs and 6-4PPs by performing immunofluorescence (IF) and compared it with local UV damage produced by

Figure 5. **Transcription dependent mobility of GFP-CSB.** (A and B) FRAP analysis of GFP-CSB, in the presence of 50 ng/ml ActD (RNAPI and RNAPII transcription inhibitor). (A) Nucleolar FRAP in absence of damages (light blue) and after damage infliction (dark blue). (B) Nucleoplasm FRAP in the presence (dark green) and absence of damage (light green). FRAP curves are from >10 cells, error bars represent SEM. FRAP curves from Fig. 4 A are in light colors for an easier comparison.



irradiation through a filter as done previously (Katsumi et al., 2001; Volker et al., 2001). For immunofluorescence (IF), cells were grown on sterile glass coverslips and immediately after DNA damage formation fixed in 2% PFA in PBS for 15 min at room temperature (RT). Permeabilization was done with 3 × 10 min incubation in PBS containing 0.1% Triton X-100. To denature DNA, 5 min RT incubation in fresh 0.07 N NaOH was done. Coverslips were subsequently washed with PBS containing 0.5% bovine serum albumin (BSA) and 0.15% glycine. Primary and secondary antibody incubation was done at RT for 2 and 1 h respectively in a humidified box in PBS with 0.5% (BSA) and 0.15% glycine. Washing of antibodies was made in PBS with 0.1% Triton X-100. Final mounting was done in Vectashield with DAPI (Vector Laboratories). To avoid any intra-experimental variation the CPD/6-4PP stainings were performed on the same coverslip with antibody TDM2 and 6-4-M2, respectively (Mori et al., 1991). The cells subjected to oxidative DNA damage infliction were protected from the UVC with a sticker positioned on the top of the microporous membrane. Polyclonal anti-rabbit primary antibodies for the detection of XPC were used (Ng et al., 2003).

Visualization of 8-oxoG local damage, of cells treated as described in DNA damage formation were fixed in acetone/methanol (1:1). Cells were air dried and rehydrated for 15 min in phosphate-buffered saline (PBS) before denaturation of DNA by incubating cells in 1.5 N HCl for 30 min at RT. Cells were washed three times in PBS and neutralized with 0.1 M Na-borate, pH 8.5, for 5 min before proceeding to the immunofluorescence protocol, according to a previously described protocol (Amouroux et al., 2010), using the mouse anti-8-oxoguanine clone N45.1 (JalCA) as a primary antibody. In brief, cells were permeabilized with PBS/0.1% Triton X-100, and then blocked for 1 h in PBS/3% BSA at 37°C before incubation with the anti-8-oxoguanine. We used required secondary antibodies (anti-mouse or -rabbit) conjugated to either Alexa Fluor 488 or Alexa Fluor 594.

Microscopic analysis

Images were recorded with a confocal microscope (LSM 510; Carl Zeiss) equipped with a 63× Plan-APO (1.4 NA) oil immersion lens (Carl Zeiss). Living cells were examined in normal culture medium and maintained at 37°C and 5% CO₂ within a large chamber including the microscope. GFP fluorescence imaging was recorded after excitation with a 488-nm argon laser, and emission light was captured behind a 505–550-nm band-pass filter; mCherry and DsRed fluorescence imaging was performed using a 561-nm laser diode, and emission light was filtered by a 585-nm long-pass filter.

Fluorescence recovery after photobleaching (FRAP)

FRAP analysis was used to measure the mobility of XPC-EGFP and CSB-EGFP as described previously (Hoogstraten et al., 2002) at high time resolution on a confocal laser-scanning microscope (LSM 510 Meta; Carl Zeiss) with some modification specified thereafter. In brief, a narrow strip spanning the nucleolus or in the nucleoplasm (80/120 × 10 pixels) of a cell was monitored every 100 ms at 1.5% laser intensity (argon laser, 488 nm line) until the fluorescence signal reached a steady level. The molecules present in the strip were then photobleached for 120 ms (or 300 ms) at the maximum laser intensity. Then recovery of fluorescence was monitored every 40 ms (or 100 ms) for ~5 s (15 or 25 s) at 1.5% laser intensity. Normalization of all FRAP data were made relative to the average prebleached fluorescence after removal of the background signal when required. The acquisition was adjusted with the time of monitoring to keep the best resolution and avoid any monitor bleaching. Images obtained were analyzed using AIM software (Carl Zeiss).

DNA damage formation

The experimental system developed to induce a local oxidative DNA damage is built on a microscope (LSM 510; Carl Zeiss) using a continuous wave

(cw) 405-nm laser light illumination. The cw 405-nm laser diode was focused through the 63× objective lens in a narrow strip in the same way as for the FRAP experiment. The power of the 405-nm laser was adjusted to 70% of the maximum power to avoid bleaching and generation of DNA damage independently of the photosensitizer. The power output of the 405-nm laser measured through the 10× lens was ~0.02–0.01 mW. Ro 19-8022 photosensitizer was a gift of F. Hoffmann-La Roche, Ltd. We used a low energy 405-nm laser to closely resemble the lamp illumination used in Will et al. (1999). The rationale is to have low energy to activate the exogenous photosensitizer Ro 19-8022, a potent type II photosensitizer, without triggering other DNA damage via other endogenous photosensitizers (Will et al., 1999; Cadet et al., 2011). The Ro 19-8022 photosensitizer was added 5 min before starting the damage formation to the desired final concentration (500 nM or 4 μM) directly into the medium by adding 1 μl of the required concentrated solution. The formation of damage was done by applying several hundred iterations to the narrow strip. We could vary the number of iterations to change the load of DNA damage in concordance with the Ro 19-8022 concentration.

Assembly kinetics quantification

Accumulation of fluorescent protein was quantified with LSM software (Carl Zeiss). Quantification was done by making a ratio of the fluorescence before and after the DNA damage formation. The first relative intensity of fluorescence is taken ~10–20 s after initiation of DNA damage infliction due to the illumination time of 20 s.

Transcription inhibition

Transcription inhibitor Actinomycin D (ActD) was used at 0.05 μg.ml⁻¹ in order to inhibit transcription of RNAPs (Perry and Kelley, 1970).

Online supplemental material

Fig. S1 shows that local irradiation with the 405-nm laser and Ro 19-8022 mainly produces 8-oxoG. UV lesions like CPDs and 6-4PP are not detected by IF. The DSB recognizer Ku-80GFP is not recruited to the local damage. Silencing of OGG1 does not abrogate the recruitment of CSB and XPC to the local damage. XRCC1 is still present 30 min after the local oxidative damage formation according to BER kinetics. Fig. S2 shows quantification of CSB and XPC, and IF of OGG1 and 8-oxoG, to oxidative DNA lesions in the nucleolus and in the nucleoplasm compartment. Formation of 8-oxoG is possible in the presence of ActD. The amount of 8-oxoG detected varies according to the 405-nm laser irradiation time and the DNA content of the damaged area. Fig. S3 shows a schematic representation of the FRAP procedure and a visual inspection of CSB-GFP recruitment in the nucleolus and in the nucleoplasm in the presence of ActD. Online supplemental material is available at <http://www.jcb.org/cgi/content/full/jcb.201205149/DC1>.

We thank Arjan Theil and Reinier van der Linden for FACS sorting assistance and the Optical Imaging Center (OIC) of the Erasmus MC for technical support with live-cell microscopy. We are grateful to Anna Campalans and J. Pablo Radicella for their comments on the manuscript.

This work was supported by a Marie Curie grant (PIEF-GA-254858) to H. Menoni, the Dutch Organization for Scientific Research grants (ZonMW TOP 912.08.031 and VIDI 917.46-364) to W. Vermeulen, and the National Institutes of Health grant (1P01AG17242-02) and the European Research Council (EUFP7) advance grant (233424) to J.H.J. Hoeijmakers.

Submitted: 23 May 2012

Accepted: 16 November 2012

References

Amouroux, R., A. Campalans, B. Epe, and J.P. Radicella. 2010. Oxidative stress triggers the preferential assembly of base excision repair complexes on open chromatin regions. *Nucleic Acids Res.* 38:2878–2890. <http://dx.doi.org/10.1093/nar/gkp1247>

Bergink, S., W. Toussaint, M.S. Luijsterburg, C. Dinant, S. Alekseev, J.H. Hoeijmakers, N.P. Dantuma, A.B. Houtsmuller, and W. Vermeulen. 2012. Recognition of DNA damage by XPC coincides with disruption of the XPC-RAD23 complex. *J. Cell Biol.* 196:681–688. <http://dx.doi.org/10.1083/jcb.201107050>

Bradsher, J., J. Auriol, L. Proietti de Santis, S. Iben, J.L. Vonesch, I. Grummt, and J.M. Egly. 2002. CSB is a component of RNA pol I transcription. *Mol. Cell.* 10:819–829. [http://dx.doi.org/10.1016/S1097-2765\(02\)00678-0](http://dx.doi.org/10.1016/S1097-2765(02)00678-0)

Cadet, J., T. Douki, and J.L. Ravanat. 2011. Measurement of oxidatively generated base damage in cellular DNA. *Mutat. Res.* 711:3–12. <http://dx.doi.org/10.1016/j.mrfmmm.2011.02.004>

Charlet-Berguerand, N., S. Feuerhahn, S.E. Kong, H. Ziserman, J.W. Conaway, R. Conaway, and J.M. Egly. 2006. RNA polymerase II bypass of oxidative DNA damage is regulated by transcription elongation factors. *EMBO J.* 25:5481–5491. <http://dx.doi.org/10.1038/sj.emboj.7601403>

Citterio, E., V. Van Den Boom, G. Schnitzler, R. Kanaar, E. Bonte, R.E. Kingston, J.H. Hoeijmakers, and W. Vermeulen. 2000. ATP-dependent chromatin remodeling by the Cockayne syndrome B DNA repair-transcription-coupling factor. *Mol. Cell. Biol.* 20:7643–7653. <http://dx.doi.org/10.1128/MCB.20.20.7643-7653.2000>

D'Errico, M., E. Parlanti, M. Teson, B.M. de Jesus, P. Degan, A. Calcagnile, P. Jaruga, M. Björås, M. Crescenzi, A.M. Pedrini, et al. 2006. New functions of XPC in the protection of human skin cells from oxidative damage. *EMBO J.* 25:4305–4315. <http://dx.doi.org/10.1038/sj.emboj.7601277>

Dianov, G., C. Bischoff, M. Sunesen, and V.A. Bohr. 1999. Repair of 8-oxoguanine in DNA is deficient in Cockayne syndrome group B cells. *Nucleic Acids Res.* 27:1365–1368. <http://dx.doi.org/10.1093/nar/27.5.1365>

Dinant, C., M. de Jager, J. Essers, W.A. van Cappellen, R. Kanaar, A.B. Houtsmuller, and W. Vermeulen. 2007. Activation of multiple DNA repair pathways by sub-nuclear damage induction methods. *J. Cell Sci.* 120:2731–2740. <http://dx.doi.org/10.1242/jcs.004523>

Gorski, S.A., S.K. Snyder, S. John, I. Grummt, and T. Misteli. 2008. Modulation of RNA polymerase assembly dynamics in transcriptional regulation. *Mol. Cell.* 30:486–497. <http://dx.doi.org/10.1016/j.molcel.2008.04.021>

Grummt, I., and A.G. Ladurner. 2008. A metabolic throttle regulates the epigenetic state of rDNA. *Cell.* 133:577–580. <http://dx.doi.org/10.1016/j.cell.2008.04.026>

Hanawalt, P.C., and G. Spivak. 2008. Transcription-coupled DNA repair: two decades of progress and surprises. *Nat. Rev. Mol. Cell Biol.* 9:958–970. <http://dx.doi.org/10.1038/nrm2549>

Hegde, M.L., T.K. Hazra, and S. Mitra. 2008. Early steps in the DNA base excision/single-strand interruption repair pathway in mammalian cells. *Cell Res.* 18:27–47. <http://dx.doi.org/10.1038/cr.2008.8>

Hoogstraten, D., A.L. Nigg, H. Heath, L.H. Mullenders, R. van Driel, J.H. Hoeijmakers, W. Vermeulen, and A.B. Houtsmuller. 2002. Rapid switching of TFIIH between RNA polymerase I and II transcription and DNA repair in vivo. *Mol. Cell.* 10:1163–1174. [http://dx.doi.org/10.1016/S1097-2765\(02\)00709-8](http://dx.doi.org/10.1016/S1097-2765(02)00709-8)

Hoogstraten, D., S. Bergink, J.M. Ng, V.H. Verbiest, M.S. Luijsterburg, B. Geverts, A. Raams, C. Dinant, J.H. Hoeijmakers, W. Vermeulen, and A.B. Houtsmuller. 2008. Versatile DNA damage detection by the global genome nucleotide excision repair protein XPC. *J. Cell Sci.* 121:2850–2859. <http://dx.doi.org/10.1242/jcs.031708>

Houtsmuller, A.B., and W. Vermeulen. 2001. Macromolecular dynamics in living cell nuclei revealed by fluorescence redistribution after photobleaching. *Histochem. Cell Biol.* 115:13–21.

Kassam, S.N., and A.J. Rainbow. 2007. Deficient base excision repair of oxidative DNA damage induced by methylene blue plus visible light in xeroderma pigmentosum group C fibroblasts. *Biochem. Biophys. Res. Commun.* 359:1004–1009. <http://dx.doi.org/10.1016/j.bbrc.2007.06.005>

Katsumi, S., N. Kobayashi, K. Imoto, A. Nakagawa, Y. Yamashina, T. Muramatsu, T. Shirai, S. Miyagawa, S. Sugiura, F. Hanaoka, et al. 2001. In situ visualization of ultraviolet-light-induced DNA damage repair in locally irradiated human fibroblasts. *J. Invest. Dermatol.* 117:1156–1161. <http://dx.doi.org/10.1046/j.0022-202x.2001.01540.x>

Khobta, A., N. Kitsera, B. Speckmann, and B. Epe. 2009. 8-Oxoguanine DNA glycosylase (Ogg1) causes a transcriptional inactivation of damaged DNA in the absence of functional Cockayne syndrome B (Csb) protein. *DNA Repair (Amst.)* 8:309–317. <http://dx.doi.org/10.1016/j.dnarep.2008.11.006>

Kirkali, G., N.C. de Souza-Pinto, P. Jaruga, V.A. Bohr, and M. Dizdaroglu. 2009. Accumulation of (5'S)-8,5'-cyclo-2'-deoxyadenosine in organs of Cockayne syndrome complementation group B gene knockout mice. *DNA Repair (Amst.)* 8:274–278. <http://dx.doi.org/10.1016/j.dnarep.2008.09.009>

Kitsera, N., D. Stathis, B. Lühnsdorf, H. Müller, T. Carell, B. Epe, and A. Khobta. 2011. 8-Oxo-7,8-dihydroguanine in DNA does not constitute a barrier to transcription, but is converted into transcription-blocking damage by OGG1. *Nucleic Acids Res.* 39:5926–5934. <http://dx.doi.org/10.1093/nar/gkr163>

Lagerwerf, S., M.G. Vrouwe, R.M. Overmeer, M.I. Fouteri, and L.H. Mullenders. 2011. DNA damage response and transcription. *DNA Repair (Amst.)* 10:743–750. <http://dx.doi.org/10.1016/j.dnarep.2011.04.024>

Lan, L., S. Nakajima, Y. Oohata, M. Takao, S. Okano, M. Masutani, S.H. Wilson, and A. Yasui. 2004. In situ analysis of repair processes for oxidative DNA damage in mammalian cells. *Proc. Natl. Acad. Sci. USA.* 101:13738–13743. <http://dx.doi.org/10.1073/pnas.0406048101>

- Lipscomb, L.A., M.E. Peek, M.L. Morningstar, S.M. Verghis, E.M. Miller, A. Rich, J.M. Essigmann, and L.D. Williams. 1995. X-ray structure of a DNA decamer containing 7,8-dihydro-8-oxoguanine. *Proc. Natl. Acad. Sci. USA.* 92:719–723. <http://dx.doi.org/10.1073/pnas.92.3.719>
- Mari, P.O., B.I. Florea, S.P. Persengiev, N.S. Verkaik, H.T. Brüngenwirth, M. Modesti, G. Giglia-Mari, K. Bezstarosti, J.A. Demmers, T.M. Luijder, et al. 2006. Dynamic assembly of end-joining complexes requires interaction between Ku70/80 and XRCC4. *Proc. Natl. Acad. Sci. USA.* 103:18597–18602. <http://dx.doi.org/10.1073/pnas.0609061103>
- Maynard, S., S.H. Schurman, C. Harboe, N.C. de Souza-Pinto, and V.A. Bohr. 2009. Base excision repair of oxidative DNA damage and association with cancer and aging. *Carcinogenesis.* 30:2–10. <http://dx.doi.org/10.1093/carcin/bgn250>
- Melis, J.P., S.W. Wijnhoven, R.B. Beems, M. Roodbergen, J. van den Berg, H. Moon, E. Friedberg, G.T. van der Horst, J.H. Hoeijmakers, J. Vijg, and H. van Steeg. 2008. Mouse models for xeroderma pigmentosum group A and group C show divergent cancer phenotypes. *Cancer Res.* 68:1347–1353. <http://dx.doi.org/10.1158/0008-5472.CAN-07-6067>
- Melis, J.P., M. Luijten, L.H. Mullenders, and H. van Steeg. 2011. The role of XPC: implications in cancer and oxidative DNA damage. *Mutat. Res.* 728:107–117. <http://dx.doi.org/10.1016/j.mrrev.2011.07.001>
- Menoni, H., D. Gasparutto, A. Hamiche, J. Cadet, S. Dimitrov, P. Bouvet, and D. Angelov. 2007. ATP-dependent chromatin remodeling is required for base excision repair in conventional but not in variant H2A.Bbd nucleosomes. *Mol. Cell. Biol.* 27:5949–5956. <http://dx.doi.org/10.1128/MCB.00376-07>
- Menoni, H., M.S. Shukla, V. Gerson, S. Dimitrov, and D. Angelov. 2012. Base excision repair of 8-oxoG in dinucleosomes. *Nucleic Acids Res.* 40:692–700. <http://dx.doi.org/10.1093/nar/gkr761>
- Mori, T., M. Nakane, T. Hattori, T. Matsunaga, M. Ihara, and O. Nikaido. 1991. Simultaneous establishment of monoclonal antibodies specific for either cyclobutane pyrimidine dimer or (6-4)photoproduct from the same mouse immunized with ultraviolet-irradiated DNA. *Photochem. Photobiol.* 54:225–232. <http://dx.doi.org/10.1111/j.1751-1097.1991.tb02010.x>
- Moriya, M. 1993. Single-stranded shuttle phagemid for mutagenesis studies in mammalian cells: 8-oxoguanine in DNA induces targeted G.C→T.A transversions in simian kidney cells. *Proc. Natl. Acad. Sci. USA.* 90:1122–1126. <http://dx.doi.org/10.1073/pnas.90.3.1122>
- Mortusewicz, O., and H. Leonhardt. 2007. XRCC1 and PCNA are loading platforms with distinct kinetic properties and different capacities to respond to multiple DNA lesions. *BMC Mol. Biol.* 8:81. <http://dx.doi.org/10.1186/1471-2199-8-81>
- Naegeli, H., and K. Sugawara. 2011. The xeroderma pigmentosum pathway: decision tree analysis of DNA quality. *DNA Repair (Amst.)*. 10:673–683. <http://dx.doi.org/10.1016/j.dnarep.2011.04.019>
- Ng, J.M., W. Vermeulen, G.T. van der Horst, S. Bergink, K. Sugawara, H. Vrieling, and J.H. Hoeijmakers. 2003. A novel regulation mechanism of DNA repair by damage-induced and RAD23-dependent stabilization of xeroderma pigmentosum group C protein. *Genes Dev.* 17:1630–1645. <http://dx.doi.org/10.1101/gad.260003>
- Oda, Y., S. Uesugi, M. Ikehara, S. Nishimura, Y. Kawase, H. Ishikawa, H. Inoue, and E. Ohtsuka. 1991. NMR studies of a DNA containing 8-hydroxydeoxyguanosine. *Nucleic Acids Res.* 19:1407–1412. <http://dx.doi.org/10.1093/nar/19.7.1407>
- Osterod, M., E. Larsen, F. Le Page, J.G. Hengstler, G.T. Van Der Horst, S. Boiteux, A. Klungland, and B. Epe. 2002. A global DNA repair mechanism involving the Cockayne syndrome B (CSB) gene product can prevent the in vivo accumulation of endogenous oxidative DNA base damage. *Oncogene.* 21:8232–8239. <http://dx.doi.org/10.1038/sj.onc.1206027>
- Perry, R.P., and D.E. Kelley. 1970. Inhibition of RNA synthesis by actinomycin D: characteristic dose-response of different RNA species. *J. Cell. Physiol.* 76:127–139. <http://dx.doi.org/10.1002/jcp.1040760202>
- Politi, A., M.J. Moné, A.B. Houtsmuller, D. Hoogstraten, W. Vermeulen, R. Heinrich, and R. van Driel. 2005. Mathematical modeling of nucleotide excision repair reveals efficiency of sequential assembly strategies. *Mol. Cell.* 19:679–690. <http://dx.doi.org/10.1016/j.molcel.2005.06.036>
- Rademakers, S., M. Volker, D. Hoogstraten, A.L. Nigg, M.J. Moné, A.A. Van Zeeland, J.H. Hoeijmakers, A.B. Houtsmuller, and W. Vermeulen. 2003. Xeroderma pigmentosum group A protein loads as a separate factor onto DNA lesions. *Mol. Cell. Biol.* 23:5755–5767. <http://dx.doi.org/10.1128/MCB.23.16.5755-5767.2003>
- Radicella, J.P., C. Dherin, C. Desmaze, M.S. Fox, and S. Boiteux. 1997. Cloning and characterization of hOGG1, a human homolog of the OGG1 gene of *Saccharomyces cerevisiae*. *Proc. Natl. Acad. Sci. USA.* 94:8010–8015. <http://dx.doi.org/10.1073/pnas.94.15.8010>
- Rosenquist, T.A., D.O. Zharkov, and A.P. Grollman. 1997. Cloning and characterization of a mammalian 8-oxoguanine DNA glycosylase. *Proc. Natl. Acad. Sci. USA.* 94:7429–7434. <http://dx.doi.org/10.1073/pnas.94.14.7429>
- Sági, J., A.B. Guliaev, and B. Singer. 2001. 15-mer DNA duplexes containing an abasic site are thermodynamically more stable with adjacent purines than with pyrimidines. *Biochemistry.* 40:3859–3868. <http://dx.doi.org/10.1021/bi0024409>
- Saxowsky, T.T., K.L. Meadows, A. Klungland, and P.W. Doetsch. 2008. 8-Oxoguanine-mediated transcriptional mutagenesis causes Ras activation in mammalian cells. *Proc. Natl. Acad. Sci. USA.* 105:18877–18882. <http://dx.doi.org/10.1073/pnas.0806464105>
- Sedelnikova, O.A., C.E. Redon, J.S. Dickey, A.J. Nakamura, A.G. Georgakilas, and W.M. Bonner. 2010. Role of oxidatively induced DNA lesions in human pathogenesis. *Mutat. Res.* 704:152–159. <http://dx.doi.org/10.1016/j.mrrev.2009.12.005>
- Shibutani, S., M. Takeshita, and A.P. Grollman. 1991. Insertion of specific bases during DNA synthesis past the oxidation-damaged base 8-oxodG. *Nature.* 349:431–434. <http://dx.doi.org/10.1038/349431a0>
- Singh, S.K., M.W. Szulik, M. Ganguly, I. Khutshivili, M.P. Stone, L.A. Marky, and B. Gold. 2011. Characterization of DNA with an 8-oxoguanine modification. *Nucleic Acids Res.* 39:6789–6801. <http://dx.doi.org/10.1093/nar/gkr275>
- Spivak, G., and P.C. Hanawalt. 2006. Host cell reactivation of plasmids containing oxidative DNA lesions is defective in Cockayne syndrome but normal in UV-sensitive syndrome fibroblasts. *DNA Repair (Amst.)*. 5:13–22. <http://dx.doi.org/10.1016/j.dnarep.2005.06.017>
- Stevnsner, T., M. Muftuoglu, M.D. Aamann, and V.A. Bohr. 2008. The role of Cockayne Syndrome group B (CSB) protein in base excision repair and aging. *Mech. Ageing Dev.* 129:441–448. <http://dx.doi.org/10.1016/j.mad.2008.04.009>
- Tornaletti, S., L.S. Maeda, R.D. Kolodner, and P.C. Hanawalt. 2004. Effect of 8-oxoguanine on transcription elongation by T7 RNA polymerase and mammalian RNA polymerase II. *DNA Repair (Amst.)*. 3:483–494. <http://dx.doi.org/10.1016/j.dnarep.2004.01.003>
- Tuo, J., C. Chen, X. Zeng, M. Christiansen, and V.A. Bohr. 2002. Functional crosstalk between hOgg1 and the helicase domain of Cockayne syndrome group B protein. *DNA Repair (Amst.)*. 1:913–927. [http://dx.doi.org/10.1016/S1568-7864\(02\)00116-7](http://dx.doi.org/10.1016/S1568-7864(02)00116-7)
- van den Boom, V., E. Citterio, D. Hoogstraten, A. Zotter, J.M. Egly, W.A. van Cappellen, J.H. Hoeijmakers, A.B. Houtsmuller, and W. Vermeulen. 2004. DNA damage stabilizes interaction of CSB with the transcription elongation machinery. *J. Cell Biol.* 166:27–36. <http://dx.doi.org/10.1083/jcb.200401056>
- Volker, M., M.J. Moné, P. Karmakar, A. van Hoffen, W. Schul, W. Vermeulen, J.H. Hoeijmakers, R. van Driel, A.A. van Zeeland, and L.H. Mullenders. 2001. Sequential assembly of the nucleotide excision repair factors in vivo. *Mol. Cell.* 8:213–224. [http://dx.doi.org/10.1016/S1097-2765\(01\)00281-7](http://dx.doi.org/10.1016/S1097-2765(01)00281-7)
- Will, O., E. Gocke, I. Eckert, I. Schulz, M. Pflaum, H.C. Mahler, and B. Epe. 1999. Oxidative DNA damage and mutations induced by a polar photosensitizer, Ro19-8022. *Mutat. Res.* 435:89–101. [http://dx.doi.org/10.1016/S0921-8777\(99\)00039-7](http://dx.doi.org/10.1016/S0921-8777(99)00039-7)
- Yuan, X., W. Feng, A. Imhof, I. Grummt, and Y. Zhou. 2007. Activation of RNA polymerase I transcription by cockayne syndrome group B protein and histone methyltransferase G9a. *Mol. Cell.* 27:585–595. <http://dx.doi.org/10.1016/j.molcel.2007.06.021>
- Zharkov, D.O., T.A. Rosenquist, S.E. Gerchman, and A.P. Grollman. 2000. Substrate specificity and reaction mechanism of murine 8-oxoguanine-DNA glycosylase. *J. Biol. Chem.* 275:28607–28617. <http://dx.doi.org/10.1074/jbc.M002441200>